J. Membrane Biol. 181, 125–135 (2001)
DOI: 10.1007/s00232-001-0016-2

The Journal of
Membrane
Biology

Inhibition of Glial Na^+ and K^+ Currents by Tamoxifen

K. A. Smitherman, H. Sontheimer
Departments of Neurobiology and Cell Biology and Medical Scientist Training Program, University of Alabama at Birmingham, Birmingham, AL 35294, USA

Received: 12 October 2000/Revised: 12 February 2001

Abstract. Tamoxifen (tmx) is a non-steroidal triphenylethylene derivative that is predominantly known as a competitive antagonist at the estrogen receptor and is used in the treatment of breast cancer. Recent studies suggest that tamoxifen is also beneficial in the treatment of brain metastases and primary brain tumors. Tmx accumulates in brain and its concentration can be up to 46-fold higher than in serum. Therefore, astrocytes may be exposed to tmx in vivo.

We use the whole-cell patch-clamp technique to examine the effects of tmx on voltage-dependent cation currents in rat cortical cultures. Using biophysical and pharmacological methods, we isolate sustained and transient outward potassium currents (I_{KS} and I_{KT}, respectively), inwardly rectifying potassium currents (I_{KIR}), and transient inward sodium currents (I_{Na}). We show that that TTX-sensitive I_{Na} is completely inhibited by 10 μM tmx within 5 min. Similarly, tmx blocks I_{KS}, but does not inhibit I_{KT} or I_{KIR} at these concentrations. Tmx effects are irreversible with 10 min wash.

Interestingly, the currents sensitive to tmx are important in growth control of glial cells (MacFarlane & Sontheimer, 1997). Therefore, we examine cytotoxic and proliferative effects of tmx. Tmx (10 μM) is not cytotoxic as judged by trypan blue exclusion. However, incubation with tmx significantly reduces cell proliferation as examined by ^{3}[H]-thymidine uptake.

Key Words: Astrocytes—Glia—Ion channels—Tamoxifen

Correspondence to: H. Sontheimer

Introduction

Tamoxifen (tmx) is a first-line systemic adjuvant therapy in the treatment of breast cancer. Tmx competitively inhibits the actions of estrogen at the estrogen receptor and provides anti-tumor effects (Jordan, 1992). However, its complete mechanism of action is more complex and not clearly delineated. Some recently identified intracellular and specific membrane effects of tmx include inhibition of protein kinase C (PKC) (O'Brian et al., 1985), inhibition of P-glycoprotein and associated volume-sensitive chloride currents (Zhang et al., 1995; Zhang et al., 1994; Valverde et al., 1996), inhibition of voltage-activated cation currents (Rouzaire-Dubois & Dubois, 1990; Hardy, deFelipe, & Valverde, 1998), and inhibition of volume-related glutamate and aspartate release (Phillis, Song, & O'Regan, 1998). These effects, possibly combined with nonspecific membrane intercalation and increased membrane stability (Wiseman et al., 1992), result in clinically important observations such as formation of cataracts (Zhang et al., 1994, 1995) and prolongation of the QT interval (Trump et al., 1992; Liu et al., 1998).

Reports indicate that overstimulation of PKC partially accounts for proliferation of malignant gliomas (*see* Bredel & Pollack, 1997; Baltuch et al., 1995 for reviews). Therefore, inhibition of PKC by tmx could be useful in treatment of brain tumors. Indeed, in vitro studies show that tmx inhibits proliferation (Weller et al., 1997; Jordan, 1992) and migration (Soroceanu, Manning, Jr., & Sontheimer, 1999) of gliomas, and several Phase I and II clinical trials for treatment of glioma and brain metastases are currently underway (Pollack et al., 1997; Mastronardi et al., 1998; Couldwell et al., 1996; Couldwell et al., 1993; Chamberlain & Kormanik, 1999; Baltuch et al., 1993). These trials involve high dose oral

therapy to achieve plasma concentrations in the micromolar range (Chamberlain & Kormanik, 1999).

Astrocytes control the brain microenvironment and any disruption of their function could result in homeostatic imbalance and brain insult. We, therefore, set out to investigate effects of tmx on astrocyte membrane properties by whole-cell patch-clamp recordings. This is the first characterization of the effects of tmx on voltage-gated channels in glial cells. We show that both voltage-activated Na^+ and sustained K^+ currents are inhibited by tmx, while other K^+ currents (transient K^+- and inwardly-rectifying K^+ currents) are not.

Materials and Methods

Cell Culture

Cortical astrocyte cultures were isolated from Sprague-Dawley rats at postnatal day 0–2 by modification of the technique described by McCarthy and deVellis (1980). The pups were placed on ice and decapitated. The brain tissue was dissected in ice-cold Earl's Minimal Essential Medium (EMEM; GIBCO, Grand Island, NY). The meninges and blood vessels were removed, and the neocortex was separated from surrounding regions. The tissue pieces were then minced, washed two times with EMEM, and placed in enzyme solution (bubbled with 100% O_2 for 10 min prior) for 20 min at 37°C. The enzyme solution consisted of EMEM supplemented with 0.5 mM EDTA, 1.65 mM L-cysteine, 706 U/ml deoxyribonuclease (Worthington, Freehold, NJ), and 30 U/ml papain (Worthington, Freehold, NJ). The cells were pelleted by centrifugation for 3 min. The supernatant was aspirated and the remaining pellet was dissociated by trituration (15–20×) with a fire-polished Pasteur pipette into astrocyte medium (~3 ml). Astrocyte medium consisted of EMEM, 10% fetal calf serum (HyClone, Logan, UT), 20 mM glucose, and 500 U/ml penicillin/streptomycin. The cells were plated at a density of ~1×10^5 cells/ml onto 12 mm coverslips coated with poly-ornithine, and then kept at 37°C in a 95% O_2/5% CO_2 atmosphere. The medium was changed every 3 days. All chemicals were Sigma-Aldrich (St. Louis, MO) products unless otherwise noted.

Electrophysiology

The whole-cell patch-clamp technique (Hamill et al., 1981) was used to obtain current recordings from cells >5 days in vitro. The patch pipettes of thin-walled borosilicate glass (TW150F-4, World Precision, Sarasota, FL) were pulled to micron diameter tips (PP-83, Narishige, Japan) with typical resistances of 2–4 MΩ when filled with KCl pipette solution (*see* Table). The pipette and bath electrodes were silver wire (AGW1010/2030, World Precision, Sarasota, FL), and the bath electrode contacted the bath solution via an agar bridge back-filled with appropriate pipette solution to minimize junction potential effects. An inverted Nikon Diaphot 200 equipped with Hoffman Modulation Contrast was used for recordings. The cells were continuously perfused at room temperature with saline solution and superfusate that allowed for fast exchange of the bath. In an attempt to isolate maximally the currents of interest, a variety of bath and pipette solutions were used, and these are summarized in the Table. The solutions were HEPES-buffered, and the pH of bath was 7.4 and of pipette was 7.3. The osmolarity of the bath solution was not adjusted for addition of drugs unless the change exceeded 5 mOsm. When appropriate, the NaCl concentration was reduced to compensate. Tmx was dissolved as stock solution in dimethyl sulphoxide (DMSO), and the final concentration of DMSO was 0.1%. This concentration of DMSO in bath solution did not affect the ionic currents of interest when applied for times used in this study (*data not shown*). All other drugs were dissolved in sterile distilled water as stock solution and stored at 4°C.

An Axopatch-1D (Axon Instruments, Foster City, CA) amplified the current recordings and low-pass filtered the signals at 2 kHz. A Digidata 1200 (Axon Instruments) interfaced to a PC-compatible computer (Dell, Austin, TX) digitized the signal on-line at 10–100 kHz. The pClamp7 (Axon Instruments) software package was used for data acquisition. Cell capacitance (C_p) and series resistance (R_s) compensation minimized voltage errors. The amplifier reading of C_p was used as the value of the whole-cell membrane capacitance; this value closely matched that calculated by uncompensated membrane test using a 5 mV pulse in Clampex. C_p was adjusted to optimal values periodically throughout recordings. Recordings were used only if R_s was <10 MΩ before activating R_s compensation (set to ~80%).

Data Analysis

Data were collected from voltage-step protocols in Clampex, and traces were analyzed using Clampfit. Leak subtraction (P/5, opposite polarity) was used in those recordings where Na^+ and K^+ currents were isolated by ion substitution. Data were plotted with Origin 5.0/6.0 (MicroCal, Northampton, MA). The membrane resistance (R_m) values were recorded directly from membrane test values in Clampex. Current amplitudes were measured in reference to holding values (−80 mV). Specific current (pA/pF) was calculated as current amplitude divided by C_p, and ionic conductance (pS) as current amplitude divided by driving force (i.e., $[I/(E - E_{rev})]$). Activation and inactivation curves were obtained by plotting peak conductance versus step or prepulse potentials, respectively. The data points were fit to the Boltzmann equation of the form $G/G_{MAX} = 1/(1+ exp[V_{1/2} - V]/k)$, with $V_{1/2}$ representing the half-maximal voltage and k representing the voltage-dependence slope. Data were reported as means ± standard error of mean (SEM) with number of cells sampled (n). Significance (p) was determined by Student's t-test for two groups of data or by analysis of variance (ANOVA) and Bonferroni correction for multiple groups of data (SPSS, Chicago, IL).

Proliferation and Cytotoxicity Assays

Cells were cultured and maintained as described above for electrophysiology.

^{3}[H]-Thymidine Incorporation

Cells were treated with either astrocyte medium and vehicle or astrocyte medium and drug for ~1 hr prior to addition of 1 μCi/ml radiolabeled thymidine. The period of thymidine pulse was 6 hr at 37°C. The "hot" medium was aspirated, and the cells were rinsed three times with cold phosphate-buffered saline (PBS, GIBCO). NaOH (0.3 N) was added for solubilization, cells were incubated for 30 min at 37°C, and HCl (0.3 N) was added for neutralization. Aliquots were removed from each sample for protein quantification (BioRad, Hercules, CA)

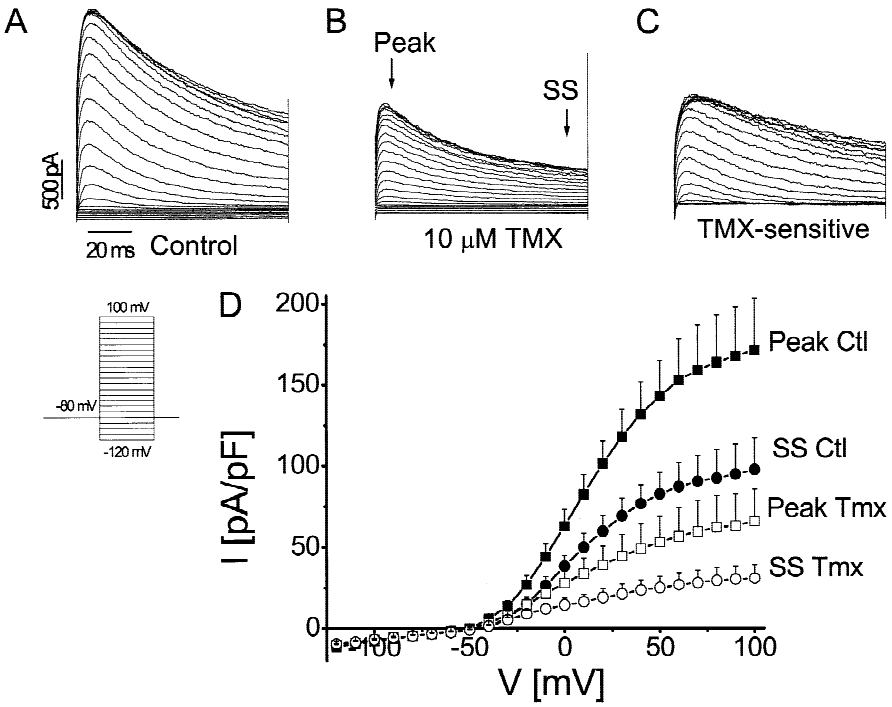

Fig. 1. Astrocytes express outwardly rectifying tmx-sensitive currents. (*A*) Representative whole-cell recordings from voltage steps from −120 mV to +100 mV for 100 msec from a −80 mV holding potential (*see* inset) under control conditions. (*B*) Voltage steps after 5 min extracellular tmx application (10 μM) show decreased current magnitudes. (*C*) Subtraction of A − B demonstrates tmx-sensitive currents. (*D*) Mean *I-V* plots of control (*Ctl*) and 5 min tmx application at peak and steady-state (*SS*) (filled squares, peak Ctl; open squares, peak tmx; filled circles, SS ctl; open circles, SS tmx).

and the remaining suspension was mixed with Scintiverse (Fisher Scientific, Springfield, NJ) for radioactivity quantification by a liquid scintillation counter (Beckman Instruments, Fullerton, CA). The data were analyzed using Excel spreadsheet (Microsoft, Redmond, WA).

Time-Lapse Photography

Time-lapse photography was used to determine cytotoxicity. 12-mm coverslips were transferred to glass bottom 35 mm dishes (MatTek Corporation, Ashland, MA), and 3 ml of astrocyte medium or astrocyte medium supplemented with 10 μM tmx was added. The dishes were placed in an LU-CB-1 tissue culture chamber (Medical Systems, Greenvale, NY) which was equipped with a 95% O_2/5% CO_2 atmosphere and an NP-2 incubator (Nikon, Japan) that was set to 37°C. The cells were visualized with an inverted Nikon Diaphot microscope and 20× phase contrast objective. The images were recorded continuously by VHS video recording and digitized every 5 min with the Axon Imaging Workbench (Axon Instruments, Foster City, CA) interfaced to a PC-compatible computer (Dell, Austin, TX).

Trypan Blue Exclusion

Trypan blue exclusion also served to determine cytotoxicity. Cells were treated with experimental conditions immediately prior to assay. The medium was aspirated, and trypan blue solution (0.1%) was added to each well for 5 min. The samples were washed two times for 3 min with PBS (GIBCO), and coverslips were mounted in Fluoromount-G (Southern Biotechnology, Birmingham, AL). Images of cell fields were captured using a charged-coupled device (Hamamatsu, Japan). The percentage of cells that excluded trypan blue determined relative cell viability.

Results

We used astrocytes from rat cortex, maintained in culture for 5–12 days, to study the effects of tmx on voltage-gated channels. These cells express voltage- and time-dependent currents characterized for each of the major ions (Bevan et al., 1985; Gray & Ritchie, 1986; Barres, Chun, & Corey, 1990). Figure 1*A* shows a representative example of recordings from cortical astrocytes in the whole-cell configuration under control conditions (*see* Table; NaCl bath and KCl pipette). We applied a family of voltage steps ranging from−120 to +100 mV in 10 mV increments from a holding potential of −80 mV (*inset*) in order to demonstrate the overall profile of inward and outward currents. Of cells recorded under control conditions ($n = 53$), recognizable current expression was as follows: inward transient (38%), outward sustained (100%), outward transient (89%), and inward rectifying (6%). The average whole-cell capacitance for these cells ($n = 103$) was 14.1 ± 0.4 pF.

Effects of tmx on Whole-Cell Currents

We initially examined the effects of tmx (10 μM) on whole-cell currents by addition to the superfusate while

Table. Composition of solutions

Concentration (mM)	Bath						Superfusate		Pipette solutions		
	NaCl	NaGluc	NMDGCl	NMDGGluc	5K+Gluc	100K+Gluc	I_{Na}	I_{KS}/I_{KT}	KCl	KGluc	NMDGGluc
Ca^{2+}	1	1	1	1	1	1	1	1	0.2	0.2	0.2
Cd^{2+}	0	0	0	0	0	0	0.5	0.5	0	0	0
Cs^{2+}	0	0	0	0	0	0	1	1	0	0	0
K^+	5	5	2	2	5	100	5	5	140	140	2
Mg^{2+}	1.2	1.2	1.2	1.2	1.2	1.2	1.2	1.2	1	1	1
Na^+	135	135	2	2	135	40	138.6	138.6	10	10	10
NMDG+	0	0	140	140	0	0	0	0	0	0	145
Cl^-	144.4	4.4	148.4	4.4	9.4	9.4	4	4	142.4	2.4	4.4
$Gluconate^-$	0	140	0	144	135	135	140	140	0	140	145
Glucose	10.5	10.5	10.5	10.5	10.5	10.5	10.5	10.5	0	0	0
EGTA	0	0	0	0	0	0	0	0	10	10	10
HEPES	32.5	32.5	32.5	32.5	32.5	32.5	32.5	32.5	10	10	10
4-AP	0	0	0	0	0	0	2	0	0	0	0
TTX (μM)	0	0	0	0	0	0	0	0.1	0	0	0

recording under control conditions. This concentration is in accordance with the plasma concentration that can be achieved with high-dose oral tmx therapy and is of the order of magnitude which affects currents in neuroblastoma cells and hypothalamic neurons (Rouzaire-Dubois & Dubois, 1990; Hardy et al. 1998). Compared to control recordings (Fig. 1*A*), exposure of cells to tmx for 5 min reduced the amplitude of the outward currents (Fig. 1*B*). Subtraction of current amplitudes after tmx exposure from control current amplitudes isolated the tmx-sensitive current (Fig. 1*C*). Figure 1*D* shows mean *I-V* plots obtained from peak and steady-state currents of cells ($n = 5$) recorded under control conditions and after exposure to 5 min tmx. The tmx-sensitive current is voltage-dependent and activates at approximately −30 mV.

To quantify the degrees of rectification under different conditions, we obtained rectification ratios by dividing the steady-state absolute current amplitude at +80 mV by that at −80 mV. Ratios greater than 1 indicate outward rectification of currents, and the magnitude of the ratios directly compares strengths of rectification. The values were 19.8 ± 3.0 for control, 6.0 ± 1.0 after 5 min tmx, and 68.6 ± 11.8 for the tmx-sensitive current. The values decreased significantly between control and 5 min tmx (paired *t*-test, $p < 0.01$, $n = 5$). Additionally, we recorded R_m directly from the membrane test value in Clampex set to average 10 pulses of +5 mV from −80 mV holding potential. R_m did not differ significantly between control and 2 min tmx exposure (*data not shown*). These data consistently suggest that tmx blocks voltage-gated currents that are active at depolarized potentials but they do not identify the specific current components that are involved.

To study the time course of tmx block, we recorded currents at specific intervals after tmx application in response to a family of voltage steps ranging from −120 mV to 100 mV in 10 mV increments from a holding potential of −80 mV (*inset*). Figure 2*A* shows mean steady-state current amplitudes at +50 mV and −50 mV for control, 2 min tmx exposure, and 5 min tmx exposure. The mean specific current values at +50 mV were 99.0 ± 12.4 pA/pF, 57.8 ± 9.2 pA/pF and 29.7 ± 8.0 pA/pF, and at −50 mV they were 4.4 ± 0.6 pA/pF, 4.5 ± 0.5 pA/pF, and 3.7 ± 0.7 pA/pF for control ($n = 8$), 2 min tmx ($n = 8$), and 5 min tmx ($n = 5$), respectively. Control values at +50 mV differed significantly from both 2 min and 5 min tmx (one-way ANOVA, $p < 0.05$), and the values at −50 mV did not differ among groups. Additionally, values at +50 mV differed between 2 min and 5 min tmx (one-way ANOVA, $p < 0.05$) and demonstrates that block of currents varies directly with length of tmx exposure. This time delay suggests that tmx may be acting indirectly, and the observed delay may reflect activation of second messenger cascades or partitioning into the cell membrane. We did not comprehensively examine such possibilities.

We tested both the reversibility and use-dependence of tmx effects. To examine reversibility, we washed cells with control bath for 10 min after tmx exposure. Specific currents at +50 mV and −50 mV of control, 2 min tmx, 5 min tmx, and wash are shown for a representative cell in Fig. 2*B*. We consistently observed little recovery towards control amplitudes when we followed tmx application with control wash. We assessed the use-dependence of block by pulsing the cell from −80 mV to +50 mV at 1 Hz for 2 min upon tmx application. At neither +50 mV nor −50 mV were current amplitudes significantly different between those cells stimulated at 1 Hz in the presence of tmx from those without stimulation. Figure 2*C* shows the mean currents from voltage steps after a 2 min tmx exposure with (*open squares*) and

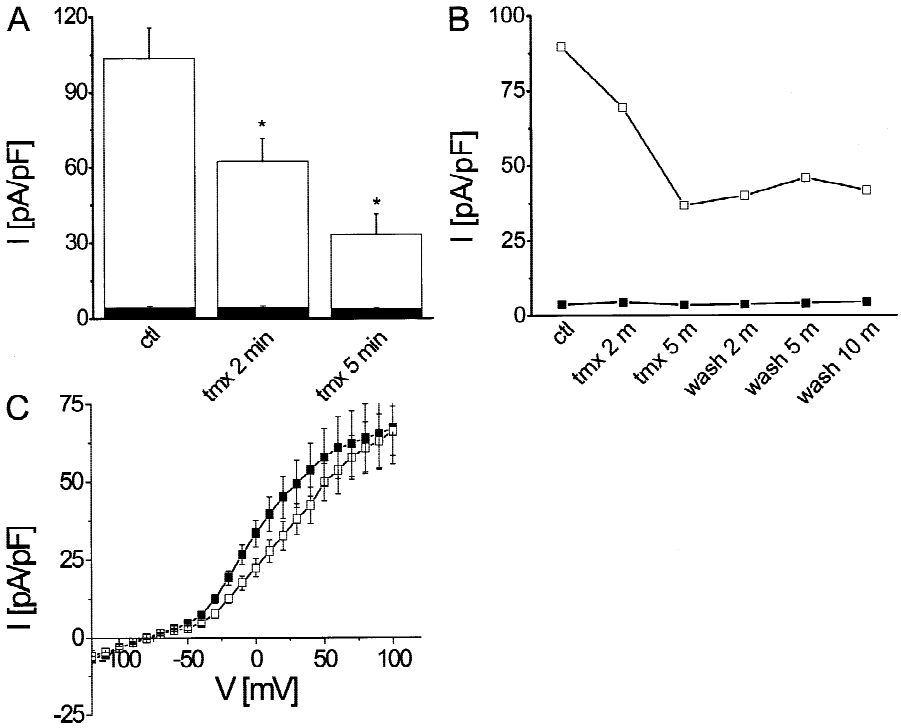

Fig. 2. Properties of tmx block. (*A*) Tmx blocks predominantly outward currents and this effect is time-dependent. The plot compares the mean +50 mV (*white*) and −50 mV (*black*) current amplitudes of control (*ctl*), 2 min tmx, and 5 min tmx. (*B*) Current amplitudes at +50 mV (open squares) and −50 mV (filled squares) for control period, tmx application, and wash-out of tmx of a representative cell. (*C*) Evaluation for use-dependence by comparing mean current amplitudes of voltage steps (*see* inset Fig. 1) after 2 min tmx exposure with (open squares) and without (filled squares) continuous 1 Hz pulse to +50 mV from a −80 mV holding potential.

without (*filled squares*) 1 Hz pulse. As control, we stimulated cells under control conditions at 1 Hz for 2 min and saw no significant decrease in amplitude (*data not shown*).

Pharmacology of tmx Block

We used a combination of biophysical and pharmacological methods to verify the ion selectivity of the tmx-sensitive current. This included ion substitution, ion channel blockers and biophysical isolation. We evaluated glial currents after bath application of 2 mM 4-aminopyridine (4-AP), 20 mM tetraethylammonium (TEA), and intracellular and extracellular *N*-Methyl D-glucamine (NMDG) substitution. 4-AP and TEA selectively block outward potassium currents (Thompson, 1977; Yeh et al., 1976a,b) and NMDG is impermeant through potassium channels. Figure 3*A* shows mean *I-V* plots from families of voltage steps (*inset*) under these conditions. Outward current amplitude is decreased with both 4-AP/TEA application and combined intracellular and extracellular NMDG substitution, and these data suggest that cells expressed typical voltage-gated potassium currents.

We examined the overlap in current sensitivity of 4-AP/TEA and NMDG to that of extracellular tmx. By first exposing cells to either 4-AP/TEA or NMDG substitution and then applying tmx, the tmx-sensitive currents were decreased (Fig. 4*B*). For each experiment, we obtained stable recordings before applying tmx. These data show that tmx-sensitive currents overlap pharmacologically with sensitivity to 4-AP/TEA and NMDG substitution and suggest that tmx blocks voltage-gated potassium currents.

Isolation of I_{KS} and I_{KT}

We specifically examined cation block by tmx with isolation solutions that are detailed in the Table. To isolate outwardly rectifying K^+ currents and to inhibit Na^+ and Ca^{2+} currents, 140 mM gluconic acid in the pipette and bath was substituted for chloride and 0.5 mM Cd^{2+}, 1 mM Cs^+, and 100 nM TTX were added to the superfusate (see NaGluc bath, I_{KS}/I_{KT} superfuse, KGluc pipette in the Table). We separated transient (I_{KT}) and sustained (I_{KS}) outward components using a voltage protocol analogous to that used by Connor & Stevens (1971). We recorded currents after hyperpolarizing (−100 mV) and depolariz-

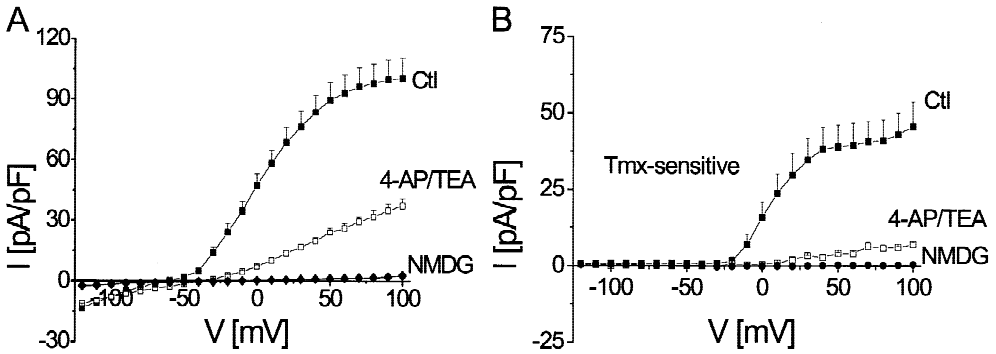

Fig. 3. Tmx-sensitive currents are sensitive to 4-AP/TEA and NMDG substitution. (*A*) Mean *I-V* plots at steady-state under different conditions obtained from voltage step protocol as in Fig. 1*A*. The conditions were control (filled squares), + 4-AP/TEA (open squares), + intracellular and extracellular NMDG substitution (filled diamonds). (*B*) Mean *I-V* plots demonstrate overlapping sensitivities to conditions in (*A*) and tmx by reduction in the magnitude of tmx-sensitive currents (filled squares, ctl + tmx; open squares, 4-AP/TEA + tmx; filled circles, intracellular and extracellular NMDG + tmx).

ing (−40 mV) prepulses (*see* insets). Both I_{KT} and I_{KS} components were present with −110 mV prepulse (Fig. 4*A*, left) but a −40 mV prepulse only activated I_{KS} (Fig. 4*A*, middle). Subtraction of recordings (−110 mV prepulse minus −40 mV prepulse) isolated I_{KT} (Fig. 4*A*, right). Figure 4*A* shows recordings from a representative cell. As clearly shown by comparison of the upper and lower traces of Fig. 4*A*, tmx selectively reduced the amplitude of the sustained component. Figure 4*B* shows the mean *I-V* plots of I_{KT} and I_{KS} using these isolation techniques.

Figure 4*C* shows mean specific current amplitudes of I_{KT} and I_{KS} isolation under control conditions and after 2 min tmx exposure at +50 mV. I_{KT} amplitudes were 60.6 ± 9.71 pA/pF and 77.47 ± 14.53 pA/pF and I_{KS} amplitudes were 38.71 ± 3.29 pA/pF and 10.48 ± 4.35 pA/pF for control and 2 min tmx exposure, respectively ($n = 3$). As suggested earlier by the traces in Fig. 4*A*, tmx significantly reduced only the sustained I_{KS} component. We were unable to obtain accurate concentration dependence curves for I_{KS} because application of tmx resulted in a time-dependent block of this current that did not stabilize (*see* Fig. 2*B*).

Isolation of I_{Na}

A proportion of cells expressed transient inward Na^+ currents (20 of 53 under control conditions). To isolate these currents, 140 mM gluconic acid in the bath was substituted for chloride, 145 mM NMDG-gluconate in the pipette was substituted for KCl, and 0.5 mM Cd^{2+}, 1 mM Cs^+, and 2 mM 4-AP were added to the superfusate (*see* NaGluc bath, I_{Na} superfuse, NMDGGluc pipette in the Table). The resultant current profile obtained by voltage steps from −80 mV to +40 mV after 200 ms prepulse to −110 mV (*inset*) is shown in the upper trace in Fig. 5*A*. The prepulse to −110 mV relieved steady-state inactivation of sodium channels. The transient inward current was blocked by 100 nM TTX (*not shown*). Tmx also abolished this current within 5 minutes (Fig. 5*A*, lower traces). Figure 5*B* shows the mean normalized currents obtained under control conditions and after 5 min tmx exposure ($n = 3$) with the protocol in Fig. 5*A* (*inset*).

Fig. 5*C* shows activation and inactivation kinetics of the isolated current. We plotted activation curves from voltage steps after a −110 mV prepulse as normalized conductances vs. membrane potential (Fig. 5*A*, *inset*). We obtained inactivation curves by varying the prepulse potentials from −120 to 0 mV and then stepping to 10 mV. We plotted normalized current values vs. membrane potential. We fit the activation and inactivation curves to the Boltzmann equation (*see* Materials and Methods). Gluconate, as used in these recordings, likely shifted the curves of activation and inactivation of Na^+ currents in the hyperpolarizing direction (Gray & Ritchie, 1986). The apparent $V_{1/2}$ of activation was −45.4 mV with a corresponding 5.2 mV change per *e*-fold, and the $V_{1/2}$ of inactivation was −67.5 mV with a corresponding 5.7 mV change per *e*-fold. Figure 5*D* compares the time course of block by TTX and tmx. The block by tmx was notably slower and suggests differences in the mechanisms of block.

Isolation of I_{KIR}

Lastly, we evaluated the effects of tmx on inwardly rectifying potassium currents (I_{KIR}). To demonstrate these currents, we applied a 200 msec prepulse to 0 mV and then stepped to negative potentials from 0 to −180 mV in 20 mV increments. Surprisingly, our cells expressed only small inward currents (~200 pA) under the imposed conditions (NaGluc bath, KGluc pipette; *see* Table) with 5 mM extracellular K^+. Previously, Ransom & Sontheimer (1995) demonstrated that the conductance of I_{KIR}

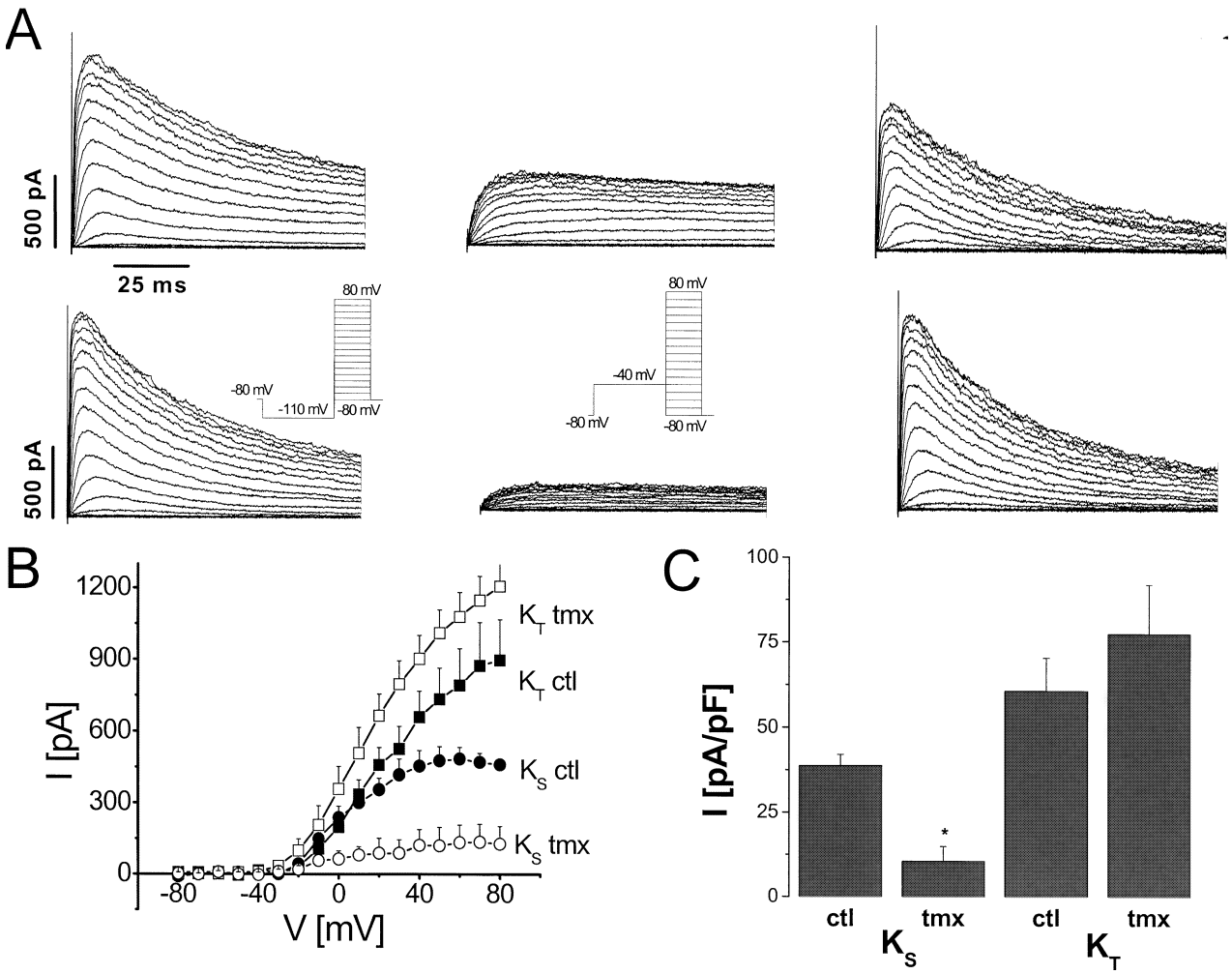

Fig. 4. Isolation of K_S and K_T currents. (*A*) Voltage-step protocols (*see* insets) and pharmacology (*see* Table) isolate the transient and sustained outward K^+ currents. The upper traces show currents in control conditions and the lower traces show the corresponding currents after 2 min extracellular tmx application for a representative cell. (*B*) Mean *I-V* plots for I_{KT} and I_{KS} obtained from the voltage-step protocols and subtraction as described for *A* (*see* text). (*C*) Comparison of current magnitudes at +50 mV in control and after 2 min extracellular tmx application for the transient and sustained K^+ currents.

increases with the square root of the extracellular K^+ concentration in spinal cord astrocytes. Therefore, we evaluated I_{KIR} with 5 mM and 100 mM extracellular K^+ (5 mM and 100 mM K^+ Gluc bath; *see* Table). Figure 6*A* shows currents recorded under 5 mM (*left*) and 100 mM (*right*) extracellular K^+. Mean *I-V* plots of these currents are given in Fig. 6*B*. These currents were sensitive to 100 μM Ba^{2+}, as previously shown (Ransom & Sontheimer, 1995). In Fig. 6*B*, we also show that 10 μM extracellular tmx has an insignificant effect on the amplitude of I_{KIR} after 5 min application. The small decrease was comparable to the decrease observed after 5 min of 100 mM K^+ without tmx (*data not shown*). In Fig. 6*C*, we plotted the mean specific currents at −140 mV for 100 mM K^+, 100 mM K^+ + 10 μM tmx, and 100 mM K^+ + 100 μM $BaCl_2$. The values were −124.4 ± 31.7 pA/pF (n = 10) for 100 K^+, −104.7 ± 18.5 pA/pF (n = 5) for 100 K^+ + 10 μM tmx, and −13.1 ± 3.6 pA/pF (n = 5) for 100 K^+ + 100 μM $BaCl_2$. Control values did not differ significantly from those after tmx application.

Cytotoxic and Anti-proliferative Effects of tmx

Several recent studies link potassium conductances to cell proliferation (Rouzaire-Dubois & Dubois, 1991; MacFarlane & Sontheimer, 1997; Knutson et al., 1997; DeCoursey et al., 1984). Specifically, the immature proliferating phenotype of astrocytes is characterized by an increase in I_{KT} and I_{KS} conductance and decreased I_{KIR} conductance when compared to the mature nonproliferative phenotype (MacFarlane & Sontheimer, 1997). In

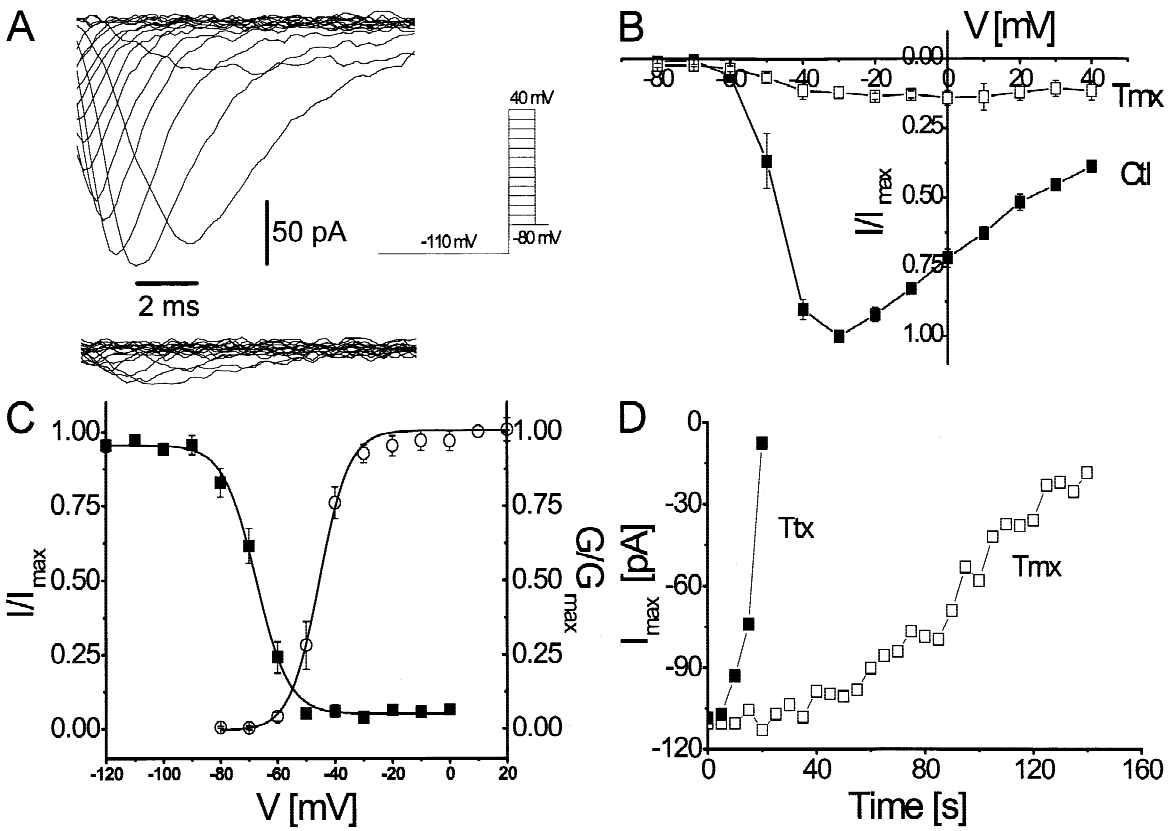

Fig. 5. Isolation of Na^+ currents. (*A*) Voltage-step protocol (*see* inset) and pharmacology (*see* Table) isolate transient inward Na^+ currents. The upper group of traces shows currents in control conditions and the lower group shows corresponding currents after 5 min extracellular tmx application for a representative cell. (*B*) Mean peak currents obtained from the voltage-step protocol shown in (*A*), in control conditions (*filled squares*) and after 5 min extracellular tmx application (*open squares*). (*C*) Activation and inactivation curves plotted under control conditions and fit to the Boltzmann equation (*see* Materials and Methods). Activation curve obtained from voltage-step protocol shown in (A) and inactivation curve obtained by stepping to +10 mV after 200 msec prepulses incremented by 10 mV from −120 mV to 0 mV. The $V_{1/2}$ of activation was −45.4 mV with a corresponding 5.2 mV change per *e*-fold. The $V_{1/2}$ of inactivation was −67.5 mV with a corresponding 5.7 mV change per *e*-fold. (*D*) Representative time course of block by tmx (open squares) and TTX (filled squares). Current magnitudes plotted for step to +10 mV after 200 msec prepulse to −110 mV every 5 sec.

agreement, Rouzaire-Dubois & Dubois (1991) demonstrate that potassium channel blockers decrease cell proliferation in neuroblastoma cells. Because tmx blocks I_{KS}, we evaluated the effect of tmx on cell proliferation in astrocytes.

Cells exposed to tmx showed a small, but significant, decrease in cell proliferation as compared to control values of ^{3}[H]-thymidine incorporation ($p < 0.01$, independent t-test, $n = 48$). Control wells averaged 20,996 ± 1,060 counts per minute, whereas wells exposed to tmx averaged 17,002 ± 847 counts per minute. We performed triplicate protein assays (*see* Materials and Methods) on each well to show that our results were not due to differences in cell number. The protein levels were similar in both groups. To further rule out any contaminating effects due to cytotoxic effects, we also performed trypan blue staining and time-lapse photography on control and tmx-exposed cells up to 12 hr. Control and tmx-exposed wells were indistinguishable suggesting that cytotoxicity does not play a role.

These experiments differed from our electrophysiological studies in that tmx added to media may be decreased to concentrations below 10 μM due to binding to serum proteins. The effective concentration could be orders of magnitude lower, as Lien et al. (1989) showed that protein binding of tmx was greater than 98% in serum. In fact, Hardy et al. (1998) showed decreased block of currents by tmx upon addition of 10% serum to the extracellular solution. Therefore, we examined ^{3}[H]-thymidine incorporation in the presence of 100 μM tmx. At this concentration, however, tmx appeared to be cytotoxic to our cells, preventing better analysis.

Discussion

This study evaluated the electrophysiological and proliferative effects of tmx on astrocytes. We demonstrated that 10 μM extracellular tmx application selectively reduced sustained outward currents by blocking voltage-

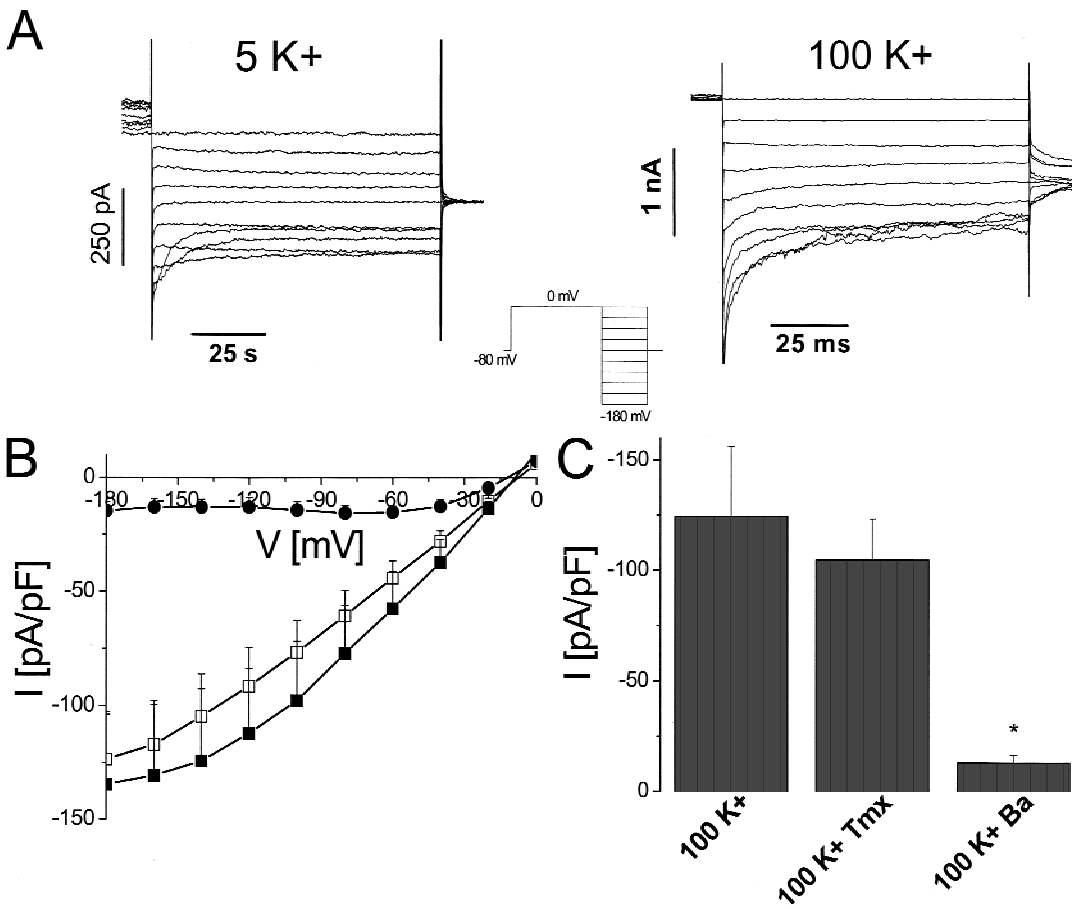

Fig. 6. Isolation of K_{IR} currents. (*A*) Voltage-step protocol (*see* inset) and pharmacology (*see* Table) isolate inwardly rectifying K^+ currents. The traces show currents in 5 mM (left) and 100 mM (right) extracellular K^+ for a representative cell. (*B*) Mean *I-V* plots of currents obtained from the voltage-step protocol in (*A*) in 100 mM extracellular K^+ (filled squares), 100 mM extracellular K^+ + 100 μM $BaCl_2$ (filled circles), and 100 mM extracellular K^+ + 10 μM tmx (open squares). (*C*) Current amplitudes at −140 mV for 100 mM extracellular K^+, 100 mM extracellular K^+ + 100 μM $BaCl_2$, and 100 mM extracellular K^+ + 10 μM tmx.

gated potassium currents. The transient outward potassium current, I_{KT}, and the inwardly rectifying potassium current, I_{KIR}, were insensitive to tmx at these concentrations. Additionally, we showed that 10 μM extracellular tmx completely blocked TTX-sensitive I_{Na}.

The physiological functions of voltage-gated currents are not well defined in nonexcitable cells, such as astrocytes. Astrocytes express two types of sodium channel, namely TTX-sensitive and TTX-resistant (Sontheimer & Waxman, 1992). The TTX-sensitive channels are similar to those that generate action potentials in excitable cells, and this type is blocked by tmx in astrocytes. Although astrocytes do not use sodium channels to produce action potentials, overlap of *h*-infinity and *m*-infinity curves suggest that sodium channels could serve other important functions (Sontheimer & Waxman, 1992). A small percentage of sodium channels should be open at resting potentials of astrocytes and could allow sufficient inward sodium flux to help the Na^+/K^+ ATPase continue its function of maintaining the resting potential. This could be important in cell cycle progression (Sontheimer et al., 1994); and the block of this process by tmx could result in disruption of cell division.

Similarly, I_{KS} could be important in general functions of the cell such as cell signaling or cell cycle control (Bevan et al., 1987). In agreement, complements of potassium channels differ with the proliferating state of astrocytes. K_S currents are upregulated in proliferating cells, whereas K_{IR} currents define the phenotype of mature, quiescent cells and are believed to mediate K^+ uptake (MacFarlane & Sontheimer, 1997). Indeed, our results demonstrated that tmx reduces proliferation in astrocytes, and this possibly could result from blocking I_{KS}.

Overall, the physiological outcome produced by blocking these channels in nonexcitable cells is not understood. However, similar voltage-gated channels are expressed in excitable cells, and they are crucial to proper physiological function. I_{Na} is responsible for the upshoot of the action potential, and I_{KS} is responsible for speeding repolarization. Our data suggest that both po-

tassium and sodium voltage-gated channels are blocked by tmx at concentrations that are attainable in patients' plasma. Blockade of these channels could result in nerve conduction failure and prolongation of the action potential duration, respectively, but such dramatic side effects are not observed clinically. In fact, the side effects of tmx are usually minimal, and the most common are hot flashes, nausea, and vomiting (Chabner et al., 1996).

Possibly, differences exist between the ability of tmx to block voltage-gated channels in nonexcitable and excitable cells, but data from other groups suggest otherwise. Liu et al. (1998) showed that I_{KS} is blocked by tmx in ventricular myocytes and Hardy et al. (1998) showed that I_{Na} is blocked by tmx in hypothalamic neurons in culture at comparable concentrations to ours. Therefore, the discrepancy may rather lie between in vitro and in vivo observations.

This work was supported by NIH grant R01-NS31234 to H. Sontheimer. K.A. Smitherman was supported by the NIH Medical Scientist Training Program.

References

Baltuch, G., Shenouda, G., Langleben, A., Villemure, J.G. 1993. High dose tamoxifen in the treatment of recurrent high grade glioma: a report of clinical stabilization and tumour regression. *Can. J. Neurol. Sci.* **20:**168–170

Baltuch, G.H., Dooley, N.P., Villemure, J.G., Yong, V.W. 1995. Protein kinase C and growth regulation of malignant gliomas. *Can. J. Neurol. Sci.* **22:**264–271

Barres, B.A., Chun, L.L.Y., Corey, D.P. 1990. Ion channels in vertebrate glia. *Annu. Rev. Neurosci.* **13:**441–474

Bevan, S., Chiu, S.Y., Gray, P.T.A., Ritchie, J.M. 1985. The presence of voltage-gated sodium, potassium and chloride channels in rat cultured astrocytes. *Proc. Roy. Soc. Lond. B:* **B225:**299–313

Bevan, S., Lindsay, R.M., Perkins, M.N., Raff, M.C. 1987. Voltage gated ionic channels in rat cultured astrocytes, reactive astrocytes and an astrocyte-oligodendrocyte progenitor cell. *J. Physiol.* (*Paris*) **82:**327–335

Bredel, M., Pollack, I.F. 1997. The role of protein kinase C (PKC) in the evolution and proliferation of malignant gliomas, and the application of PKC inhibition as a novel approach to anti-glioma therapy. *Acta Neurochir.* (*Wien*). **139:**1000–1013

Chabner, B.A., Allegra, C.J., Curt, G.A., Calabresi, P. 1996. Antineoplastic Agents. *In:* Goodman's and Gilman's The Pharmacological Basis of Therapeutics. J.G. Hardman & L.E. Limbird, editors-in-chief. p. 1275. McGraw-Hill, New York

Chamberlain, M.C., Kormanik, P.A. 1999. Salvage chemotherapy with tamoxifen for recurrent anaplastic astrocytomas. *Arch. Neurol.* **56:**703–708

Connor, J.A., Stevens, C.F. 1971. Voltage clamp studies of a transient outward membrane current in gastropod neural somata. *J. Physiol.* **213:**21–30

Couldwell, W.T., Weiss, M.H., DeGiorgio, C.M., Weiner, L.P., Hinton, D.R., Ehresmann, G.R., Conti, P.S., Apuzzo, M.L. 1993. Clinical and radiographic response in a minority of patients with recurrent malignant gliomas treated with high-dose tamoxifen. *Neurosurgery* **32:**485–489; discussion 489–490

Couldwell, W.T., Hinton, D.R., Surnock, A.A., DeGiorgio, C.M., Weiner, L.P., Apuzzo, M.L., Masri, L., Law, R.E., Weiss, M.H. 1996. Treatment of recurrent malignant gliomas with chronic oral high-dose tamoxifen. *Clin. Cancer Res.* **2:**619–622

DeCoursey, T.E., Chandy, G., Gupta, S., Cahalan, M.D. 1984. Voltage-gated K^+ channels in human T lymphocytes: a role in mitogenesis? *Nature* **307:**465–468

Gray, P.T., Ritchie, J.M. 1986. A voltage-gated chloride conductance in rat cultured astrocytes. *Proc. Roy. Soc. Lond. B:* **228:**267–288

Hamill, O.P., Marty, A., Neher, E., Sakmann, B., Sigworth, F.J. 1981. Improved patch-clamp techniques for high-resolution current recording from cells and cell-free membrane patches. *Pfluegers Arch.* **391:**85–100

Hardy, S.P., deFelipe, C., Valverde, M.A. 1998. Inhibition of voltage-gated cationic channels in rat embryonic hypothalamic neurones and C1300 neuroblastoma cells by triphenylethylene antioestrogens. *FEBS Lett.* **434:**236–240

Jordan, V.C. 1992. Overview from the International Conference on Long-Term Tamoxifen Therapy for Breast Cancer. *J. Natl. Cancer Inst.* **84:**231–234

Knutson, P., Ghiani, C.A., Zhou, J.M., Gallo, V., McBain, C.J. 1997. K^+ channel expression and cell proliferation are regulated by intracellular sodium and membrane depolarization in oligodendrocyte progenitor cells. *J. Neurosci.* **17:**2669–2682

Lien, E.A., Solheim, E., Lea, O.A., Lundgren, S., Kvinnsland, S., Ueland, P.M. 1989. Distribution of 4-hydroxy-N-desmethyltamoxifen and other tamoxifen metabolites in human biological fluids during tamoxifen treatment. *Cancer Res.* **49:**2175–2183

Liu, X.K., Katchman, A., Ebert, S.N., Woosley, R.L. 1998. The antiestrogen tamoxifen blocks the delayed rectifier potassium current, IKr, in rabbit ventricular myocytes. *J. Pharmacol. Exp. Ther.* **287:**877–883

MacFarlane, S.N., Sontheimer, H. 1997. Electrophysiological changes that accompany reactive gliosis in vitro. *J. Neurosci.* **17:**7316–7329

Mastronardi, L., Puzzilli, F., Couldwell, W.T., Farah, J.O., Lunardi, P. 1998. Tamoxifen and carboplatin combinational treatment of high-grade gliomas. Results of a clinical trial on newly diagnosed patients. *J. Neurooncol.* **38:**59–68

McCarthy, K.D., deVellis, J. 1980. Preparation of separate astroglial and oligodendroglial cell cultures from rat cerebral tissue. *J. Physiol.* **85:**890–902

O'Brian, C.A., Liskamp, P.M., Solomon, D.H., Weinstein, I.B. 1985. Inhibition of protein kinase C by tamoxifen. *Cancer Res.* **45:**2462–2465

Phillis, J.W., Song, D., O'Regan, M.H. 1998. Tamoxifen, a chloride channel blocker, reduces glutamate and aspartate release from the ischemic cerebral cortex. *Brain Res.* **780:**352–355

Pollack, I.F., DaRosso, R.C., Robertson, P.L., Jakacki, R.L., Mirro, J.R., Jr., Blatt, J., Nicholson, S., Packer, R.J., Allen, J.C., Cisneros, A., et al. 1997. A phase I study of high-dose tamoxifen for the treatment of refractory malignant gliomas of childhood. *Clin. Cancer Res.* **3:**1109–1115

Ransom, C.B., Sontheimer, H. 1995. Biophysical and pharmacological characterization of inwardly rectifying K^+ currents in rat spinal cord astrocytes. *J. Neurophysiol.* **73:**333–345

Rouzaire-Dubois, B., Dubois, J.M. 1990. Tamoxifen blocks both proliferation and voltage-dependent K^+ channels of neuroblastoma cells. *Cell Signal.* **2:**387–393

Rouzaire-Dubois, B., Dubois, J.M. 1991. A quantitative analysis of the role of K^+ channels in mitogenesis of neuroblastoma cells. *Cell Signal.* **3:**333–339

Sontheimer, H., Fernandez-Marques, E., Ullrich, N., Pappas, C.A., Waxman, S.G. 1994. Glial Na^+ channel are required for maintenance of Na+/K+-ATPase activity. *J. Neurosci.* **14:**2464–2475

Sontheimer, H., Waxman, S.G. 1992. Ion channels in spinal cord astrocytes in vitro: II. Biophysical and pharmacological analysis of two Na^+ current types. *J. Neurophysiol.* **68:**1001–1011

Soroceanu, L., Manning, T.J., Jr., Sontheimer, H. 1999. Modulation of glioma cell migration and invasion using Cl(−) and K(+) ion channel blockers. *J. Neurosci.* **19:**5942–5954

Thompson, S.H. 1977. Three pharmacologically distinct potassium channels in molluscan neurones. *J. Physiol.* **265:**465–488

Trump, D.L., Smith, D.C., Ellis, P.G., Rogers, M.P., Schold, S.C., Winer, E.P., Panella, T.J., Jordan, V.C., Fine, R.L. 1992. High-dose tamoxifen, a potential multidrug-resistance-reversal agent: phase I trial in combination with vinblastine. *J. Natl. Cancer Inst.* **84:**1811–1816

Valverde, M.A., Bond, T.D., Hardy, S.P., Taylor, J.C., Higgins, C.F., Altamirano, J., Alvarez-Leefmans, F.J. 1996. The multidrug resistance P-glycoprotein modulates cell regulatory volume decrease. *EMBO J.* **15:**4460–4468

Weller, M., Trepel, M., Grimmel, C., Schabet, M., Bremen, D., Krajewski, S., Reed, J.C. 1997. Hypericin-induced apoptosis of human malignant glioma cells is light-dependent, independent of bcl-2 expression, and does ot require wild-type p53. *Neurol. Res.* **19:**459–470

Wiseman, H., Cannon, M., Arnstein, H.R., Barlow, D.J. 1992. The structural mimicry of membrane sterols by tamoxifen: evidence from cholesterol coefficients and molecular-modelling for its action as a membrane anti-oxidant and an anti-cancer agent. *Biochim. Biophys. Acta* **1138:**197–202

Yeh, J.Z., Oxford, G.S., Wu, C.H., Narahashi, T. 1976a. Interactions of aminopyridines with potassium channels of squid axon membranes. *Biophys. J.* **16:**77–81

Yeh, J.Z., Oxford, G.S., Wu, C.H., Narahashi, T. 1976b. Dynamics of aminopyridine block of potassium channels in squid axon membrane. *J. Gen. Physiol.* **68:**519–535

Zhang, J.J., Jacob, T.J., Valverde, M.A., Hardy, S.P., Mintenig, G.M., Sepulveda, F.V., Gill, D.R., Hyde, S.C., Trezise, A.E., Higgins, C.F. 1994. Tamoxifen blocks chloride channels. A possible mechanism for cataract formation. *J. Clin. Invest.* **94:**1690–1697

Zhang, J.J., Jacob, T.J., Hardy, S.P., Higgins, C.F., Valverde, M.A. 1995. Lens opacification by antioestrogens: tamoxifen vs ICI 182,780. *Br. J. Pharmacol.* **115:**1347–1348